

Electron-deuteron scattering in a current-conserving description of relativistic bound states: including meson-exchange-current contributions

D. R. Phillips^{a,b}, S. J. Wallace^b, N. K. Devine^c

^aDepartment of Physics, University of Washington, Box 351560, Seattle, Washington 98195-1560

^bDepartment of Physics, University of Maryland, College Park, Maryland 20742-4111

^cGeneral Sciences Corporation, 4600 Powder Mill Rd., Suite 400, Beltsville, Maryland 20705-1675

Using a three-dimensional formalism that includes relativistic kinematics, the effects of negative-energy states, approximate boosts of the two-body system, and current conservation we calculate the electromagnetic form factors of the deuteron up to $Q^2 = 6 \text{ GeV}^2$. This is done both in impulse approximation and with a $\rho\pi\gamma$ meson-exchange current included. The experimentally-measured quantities A , B , and T_{20} are calculated over the kinematic range probed in recent Jefferson Laboratory experiments. The meson-exchange current provides significant strength in A at large Q^2 , but has little impact on B or T_{20} .

Theoretically the presence of a D-state in the deuteron means that three independent form factors can be constructed: the charge, magnetic, and quadrupole deuteron form factors, F_C , F_M , and F_Q . These are related to the Breit frame matrix elements of the deuteron electromagnetic current operator \mathcal{A}_μ in the three deuteron magnetic sub-states $|+1\rangle$, $|0\rangle$, and $|-1\rangle$ via the formulae:

$$F_C = \frac{1}{3\sqrt{1+\eta}e} (\langle 0|\mathcal{A}_0|0\rangle + 2\langle +1|\mathcal{A}_0|+1\rangle), \quad (1)$$

$$F_Q = \frac{1}{2\eta\sqrt{1+\eta}e} (\langle 0|\mathcal{A}_0|0\rangle - \langle +1|\mathcal{A}_0|+1\rangle), \quad (2)$$

$$F_M = \frac{-1}{\sqrt{2\eta(1+\eta)}e} \langle +1|\mathcal{A}_+|0\rangle, \quad (3)$$

with $\eta = -Q^2/(4M_d^2)$, and Q^2 the square of the four-momentum transfer to the deuteron. Hence three experimental quantities are required to disentangle the full electromagnetic structure of this nucleus. Two of these—the structure functions A and B —can be obtained from the electron-deuteron differential cross-section using the usual Rosenbluth separation. These are related to F_C , F_Q , and F_M , as follows:

$$A = F_C^2 + \frac{8}{9}\eta^2 F_Q^2 + \frac{2}{3}\eta F_M^2, \quad (4)$$

$$B = \frac{4}{3}\eta(1+\eta)F_M^2. \quad (5)$$

The third observable of choice is T_{20} , the tensor-polarization observable for electron-deuteron scattering. To obtain T_{20} electrons are scattered from a polarized deuteron target. T_{20} is the ratio of a combination of differential cross-sections for electron-deuteron scattering in the three deuteron magnetic sub-states to the unpolarized cross-section. It is related to F_C , F_Q and F_M , by:

$$T_{20} = -\sqrt{2} \frac{x(x+2) + y/2}{1 + 2(x^2 + y)}; \quad (6)$$

where

$$x = \frac{2\eta F_Q}{3F_C}; \quad y = \frac{2\eta}{3} \left[\frac{1}{2} + (1+\eta) \tan^2 \left(\frac{\theta_e}{2} \right) \right] \frac{F_M^2}{F_C^2}. \quad (7)$$

Recent experiments at the Thomas Jefferson National Accelerator Facility (JLab) have probed the electromagnetic form factors of the deuteron at large space-like momentum transfers. T_{20} has been measured at Q^2 up to almost 2 GeV^2 , B out to about 1.3 GeV^2 , and A to $Q^2 = 6 \text{ GeV}^2$. At these momentum transfers relativistic kinematics and dynamics would appear to be a necessary ingredient of any theoretical description. Hence there has been considerable effort invested in the construction of relativistic formalisms for the NN bound state. If the constituents of the bound state are understood to be the neutron and the proton then this approach is a logical extension of the standard nonrelativistic treatment of the NN system. Furthermore, regardless of the momentum transfer involved, it is crucial that the consequences of electromagnetic gauge invariance be incorporated in the calculation. Minimally this means that the electromagnetic current of the deuteron must be conserved. Indeed, the derivation of Eqs. (1)-(3) assumed that the deuteron current \mathcal{A}_μ was conserved.

Naturally, A , B , and T_{20} can be calculated using a non-relativistic NN interaction which is fit to the NN scattering data. This approach has met with a significant amount of success (see, e.g. Refs. [1,2]). In this note we report on an attempt to imitate this approach using a relativistic formalism. To this end we construct an NN interaction, place it in a relativistic scattering equation, and fit the parameters of our interaction to NN data. The electromagnetic form factors of the deuteron predicted by this NN model are then calculated. The approach includes relativistic kinematics, negative-energy states, boost effects, and relativistic pieces of the electromagnetic current explicitly at all stages of the calculation. This three-dimensional (3D) technique has been developed and applied in Refs. [3–5]. Here our focus is on elastic electron-deuteron scattering. First, we give a brief review of our formalism in which we display expressions for the bound-state equation and the current matrix element in the case of an instantaneous two-body interaction. Second, we discuss the inclusion of meson-exchange-current (MEC) contributions, especially the $\rho\pi\gamma$ MEC, which is known to give significant

contributions to electron-deuteron scattering. Then, we present our results for A , B , and T_{20} . While T_{20} is reproduced quite well there is significant discrepancy between our calculation and the experimental data for A and B .

A number of alternative 3D relativistic treatments of deuteron dynamics exist (see, for instance, Refs. [6–10]). Of these, the closest to this work is that of Hummel and Tjon [7], although we eliminate some approximations made there. Also, we do not include the $\omega\sigma\gamma$ MEC in our calculation. Our impulse approximation results are very similar to those of Ref. [7].

Consider the Bethe-Salpeter equation (BSE) for a bound-state vertex function, Γ :

$$\Gamma = KG_0\Gamma. \quad (8)$$

Here K is, in principle, the sum of all two-particle-irreducible $NN \rightarrow NN$ graphs. The NN propagator G_0 is the product of spin-half Feynman propagators for each nucleon: $G_0 = id_1d_2$. In studies of this equation for the deuteron bound state [11] the kernel K included a set of single-boson exchanges—in analogy to many non-relativistic potential models—yielding the “ladder” approximation. However, it is well known that in such an approximation the Bethe-Salpeter equation does not give the correct one-body limit [12]. In other words, if we consider unequal-mass particles, and take one of them to be very heavy, Eq. (8) does not become the Dirac equation for the light particle moving in the static field of the heavy one. This limit is only properly treated in Eq. (8) if the full set of ladder and crossed-ladder graphs is taken for K [12]. In Ref. [3] we attempted to remedy this, and showed that the pieces of the graphs which appear in K and are responsible for the one-body limit can be resummed so that Eq. (8) becomes:

$$\Gamma = U(G_0 + G_C)\Gamma, \quad (9)$$

where the precise form of G_C was derived in [3,5]. For exact correspondence between (8) and (9) we should have:

$$K = U + UG_CK. \quad (10)$$

At the level of the one-boson-exchange interaction, where K and U have only their lowest-order pieces, we see that Eq. (9) defines an improved “ladder” Bethe-Salpeter equation, which *does* have the correct one-body limit:

$$\Gamma = K^{(2)}(G_0 + G_C)\Gamma. \quad (11)$$

This equation is still four-dimensional. One straightforward way to reduce it to three dimensions is to follow Salpeter [13] and assume an instantaneous interaction, i.e. make the replacement:

$$K^{(2)}(q) = \frac{1}{q^2 - \mu^2} \quad \longrightarrow \quad K_{\text{inst}}^{(2)}(\mathbf{q}) = -\frac{1}{\mathbf{q}^2 + \mu^2}, \quad (12)$$

where $q = (q_0, \mathbf{q})$ is the four-momentum of the meson. Since $K_{\text{inst}}^{(2)}$ depends only on the three-vector \mathbf{q} this

approximation reduces Eq. (11) to a three-dimensional equation:

$$\Gamma_{\text{inst}} = K_{\text{inst}}^{(2)}\langle G_0 + G_C \rangle \Gamma_{\text{inst}}. \quad (13)$$

Here the three-dimensional propagator $\langle G_0 + G_C \rangle$ is obtained by integrating over the time-component of relative four-momentum:

$$\langle G_0 + G_C \rangle = \int \frac{dp_0}{2\pi} [G_0(p; P) + G_C(p; P)]. \quad (14)$$

Hereafter we always denote integration over zeroth components of relative four-momenta by angled brackets.

Before examining $\langle G_0 + G_C \rangle$, consider the more standard equal-time Green’s function [14,15]:

$$\langle G_0 \rangle = \frac{\Lambda_1^+ \Lambda_2^+}{E^+ - \epsilon_1 - \epsilon_2} - \frac{\Lambda_1^- \Lambda_2^-}{E^- + \epsilon_1 + \epsilon_2}; \quad (15)$$

where Λ^\pm are related to projection operators onto positive and negative-energy states of the Dirac equation, E is the total energy, and $\epsilon_i = (\mathbf{p}_i^2 + m_i^2)^{1/2}$. The propagator $\langle G_0 \rangle$ is not invertible [16], since it has no components in the $+-$ and $-+$ sectors. This is related to the lack of a correct one-body limit in the ladder BSE. If we had applied the 3D reduction (12) to Eq. (8) we would have obtained the Salpeter equation, with the non-invertible $\langle G_0 \rangle$ in the intermediate state. However, adding $\langle G_C \rangle$, which comes from resumming pieces of the crossed-ladder graphs *before* reducing to three dimensions, gives a 3D NN propagator:

$$\langle G_0 + G_C \rangle = \frac{\Lambda_1^+ \Lambda_2^+}{E^+ - \epsilon_1 - \epsilon_2} - \frac{\Lambda_1^+ \Lambda_2^-}{2\kappa_2^0 - E + \epsilon_1 + \epsilon_2} - \frac{\Lambda_1^- \Lambda_2^+}{E - 2\kappa_2^0 + \epsilon_1 + \epsilon_2} - \frac{\Lambda_1^- \Lambda_2^-}{E^- + \epsilon_1 + \epsilon_2}, \quad (16)$$

with κ_2^0 a parameter that enters through the construction of G_C . This three-dimensional propagator was derived by Mandelzweig and Wallace with κ_2^0 equal to the on-shell energy of particle two [17]. With κ_2^0 chosen in this way $\langle G_0 + G_C \rangle$ has the correct one-body limits as either particle’s mass tends to infinity and also is invertible.

In this work we consider the interaction of two particles of equal mass, and thus choose a different κ_2^0 , namely $\kappa_2^0 = (E - \epsilon_1 + \epsilon_2)/2$. This form avoids the appearance of unphysical singularities when electron-deuteron scattering is calculated [5]. It yields a two-body propagator:

$$\langle G_0 + G_C \rangle = \frac{\Lambda_1^+ \Lambda_2^+}{E^+ - \epsilon_1 - \epsilon_2} - \frac{\Lambda_1^+ \Lambda_2^-}{2\epsilon_2} - \frac{\Lambda_1^- \Lambda_2^+}{2\epsilon_1} - \frac{\Lambda_1^- \Lambda_2^-}{E^- + \epsilon_1 + \epsilon_2}, \quad (17)$$

which is consistent with that demanded by low-energy theorems for composite spin-half particles in scalar and vector fields [18]. Alternatively, comparing the $++ \rightarrow ++$ piece of

$$K_{\text{inst}}^{(2)} \langle G_0 + G_C \rangle K_{\text{inst}}^{(2)} \quad (18)$$

with the amplitude obtained at fourth order in the full 4D field theory we see that the contribution of negative-energy states agrees at leading order in $1/M$ [5]. In other words, effects such as Fig. 1 are included in a bound-state calculation that employs Eq. (13). This is true even if only the instantaneous ladder kernel $K_{\text{inst}}^{(2)}$ is used, because of our careful treatment of the one-body limit.

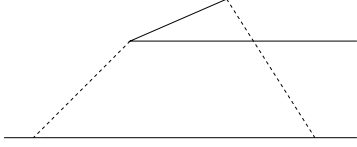


FIG. 1. One example of a Z-graph which is included in our 3D equation (13).

Of course, the instant approximation which led to Eq. (13) is uncontrolled. However, one of the central results of Ref. [3] was that similar three-dimensional reductions could be implemented in a systematically-improvable way. The numerical work of Ref. [5] then showed that the replacement of Eq. (12) by the systematic 3D reductions developed in Ref. [3] had little impact on the deuteron electromagnetic form factors. Hence in this work we will report only on results obtained using Eq. (13), even though “better” treatments of the reduction to three dimensions are certainly possible.

It remains to construct a conserved electromagnetic deuteron current. We begin by defining $\mathcal{A}_\mu^{(0)}$, the impulse approximation current obtained when the ladder Bethe-Salpeter equation (8) is solved:

$$\mathcal{A}_\mu^{(0)} = i \bar{\Gamma}(P+Q) d_1(p_1) d_2(p_2+Q) j_\mu^{(2)} d_2(p_2) \Gamma(P) + (1 \leftrightarrow 2), \quad (19)$$

where Γ is the solution of Eq. (8), $P = p_1 + p_2$ and $P+Q$ are the four-momenta of the initial and final states, and $j_\mu^{(n)}$ is the usual one-nucleon current for particle n :

$$j_\mu^{(n)} = q_n \left[F_1^{(n)}(Q^2) \gamma_\mu^{(n)} + F_2^{(n)}(Q^2) \frac{i}{2M} \sigma_{\mu\nu}^{(n)} Q^\nu \right] \quad (20)$$

(q_n is the charge). Using the Ward-Takahashi identity associated with formally-modified but practically-identical form of this current [19] it is easy to show that $\mathcal{A}_\mu^{(0)}$ is conserved, i.e.

$$Q^\mu \mathcal{A}_\mu^{(0)} = 0. \quad (21)$$

However, in this work we did not begin with the ladder BSE. Instead we began with the 4D equation (9). Constructing a conserved impulse approximation current for the vertex function which is the solution of Eq. (9) is a little more involved. In Ref. [5] we showed how to add a piece to the current (19) which results in \mathcal{A}_μ being conserved if Γ is the solution of Eq. (9):

$$\mathcal{A}_\mu = \mathcal{A}_\mu^{(0)} + \bar{\Gamma}(P+Q) G_C \Gamma(P). \quad (22)$$

The explicit expression for G_C can be found in Ref. [5].

With this four-dimensional current in hand we may make a reduction of it to three dimensions in an analogous fashion to the reduction employed for the bound-state equation itself. Once again, this reduction can be performed in a systematic fashion, but here we need only the results for an instantaneous interaction. In that case the “instant” current:

$$\mathcal{A}_{\text{inst},\mu} = \bar{\Gamma}_{\text{inst}} \mathcal{G}_{\text{inst},\mu}^\gamma \Gamma_{\text{inst}} \quad (23)$$

is conserved, provided that Γ_{inst} is the solution of Eq. (13). The explicit form of the current employed is [5]:

$$\mathcal{G}_{\text{inst},\mu}^\gamma(\mathbf{p}_1, \mathbf{p}_2; P, Q) = i \langle d_1(p_1) d_2(p_2+Q) j_\mu^{(2)} d_2(p_2) \rangle + i \langle d_1(p_1) d_2^c(p_2+Q) j_{c,\mu}^{(2)} d_2^c(p_2) \rangle + (1 \leftrightarrow 2). \quad (24)$$

Here d_n is the Dirac propagator for particle n , and $j_\mu^{(n)}$ is the one-body current (20). Only the γ^μ piece of $j_\mu^{(n)}$ is relevant for charge conservation, since the piece proportional to $\sigma^{\mu\nu}$ is automatically conserved. Meanwhile, d_n^c is a one-body Dirac propagator used in $G_C(P)$ to construct the approximation to the crossed-ladder graphs. Correspondingly, d_n^c appears in $G_C(P+Q)$. It does *not* equal d_n^c , even if particle n is not the nucleon struck by the photon. Finally,

$$j_{c,\mu}^{(2)} = (q_2 \gamma_\mu^{(2)} - \tilde{j}_\mu^{(2)}); \quad \tilde{j}_\mu^{(2)} = q_2 \frac{\hat{p}_{2\mu}' + \hat{p}_{2\mu}}{\epsilon_2' + \epsilon_2} \gamma_0^{(2)}, \quad (25)$$

with $\hat{p}_2 = (\epsilon(\mathbf{p}_2), \mathbf{p}_2)$. The current defined by Eqs. (23)–(25) includes not only the effects of time-ordered graphs like that on the left-hand side of Fig. 2, but also the effects of photons coupling to the Z-graph in Fig. 1.

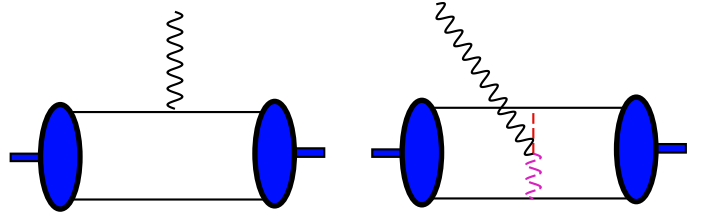


FIG. 2. On the left we depict the positive-energy-state impulse approximation mechanism for electron-deuteron scattering. On the right the $\rho\pi\gamma$ MEC diagram is shown.

This defines our impulse-approximation current. Detailed results for this current employed with the solutions of Eq. (13) were presented in Ref. [5]. In this work we move beyond the impulse approximation by including the effects of the $\rho\pi\gamma$ meson-exchange current. Because of the quantum numbers of the deuteron this is generally thought to be the lowest-mass mesonic excitation which makes a contribution to the electromagnetic deuteron current. However, note that there are additional pionic currents which should be included because

we have chosen pseudovector pion coupling. In nonrelativistic approaches pseudovector pion coupling implies that there is a “relativistic” two-body contribution to the deuteron’s charge operator involving a $\gamma\pi$ contact term [20]. In A this effect plays a more significant role than the $\rho\pi\gamma$ MEC [21]. This dynamics appears in the current operator of the formalism derived in Ref. [4], but we have not included it in this calculation.

The Lagrangian governing the $\rho\pi\gamma$ vertex is:

$$\mathcal{L} = -e \frac{g_{\rho\pi\gamma}}{2m_\rho} \epsilon_{\alpha\beta\gamma\delta} F^{\alpha\beta} \vec{\rho}^\gamma \cdot \partial^\delta \vec{\pi}. \quad (26)$$

This yields the two-body current depicted on the right-hand side of Fig. 2. In calculating this diagram the same form factors are employed at the πNN and ρNN vertices as were used in calculating the NN potential. The $\rho\pi\gamma$ current is automatically conserved.

With all the theoretical pieces of the puzzle assembled we now calculate electron-deuteron scattering. The vertex functions employed are the ones calculated with all positive and negative-energy states included, as described in Ref. [5]. If the negative-energy states are dropped the interaction is exactly the Bonn-B potential for the Thompson equation, as derived and fitted to NN phase shifts in Ref. [22]. This model gives a reasonable fit to the NN data, and good deuteron static properties, although it is not as good a fit as some more recent NN potentials [2,23,24]. When negative-energy states are included the deuteron pole position changes slightly. To compensate for this we adjust the σ -meson coupling from the value of the fit in Ref. [22], $\frac{g_\sigma^2}{4\pi} = 8.08$, to $\frac{g_\sigma^2}{4\pi} = 8.55$.

The single-nucleon form factor parametrization chosen is that of Mergell *et al.* [25]. This parametrization is based on vector-meson dominance with constraints imposed on the asymptotic shape of F_1 and F_2 using arguments from perturbative QCD.

The only remaining freedom in the calculation is the choice of the parameters governing the $\rho\pi\gamma$ MEC. The coupling $g_{\rho\pi\gamma} = 0.563$ is extracted from the decay $\rho \rightarrow \pi\gamma$. The contribution of the MEC to electron-deuteron scattering depends crucially on the behavior of the current operator as a function of Q^2 . In the work of Hummel and Tjon vector-meson dominance was used to obtain a $\rho\pi\gamma$ form factor given solely by the ω meson: $F_{\rho\pi\gamma}(Q^2) = \frac{1}{Q^2 - m_\omega^2}$. This same $\rho\pi\gamma$ form factor is also employed in the non-relativistic calculations of Refs. [1,2]. Other calculations have used form factors based on quark models [8]. Such form factors tend to reduce the contribution of this MEC, which is also very sensitive to the cutoff masses in the πNN and ρNN vertices.

In Fig. 3 we present our results for A . The left panel shows the results up to $Q^2 \approx 2 \text{ GeV}^2$ and the right panel gives results and data over the full range of experimental Q^2 . The two JLab experiments which have produced data for A [A198, A98] are denoted by triangles and squares respectively. Note that these experiments confirm the trend of the SLAC data of Arnold *et al.*

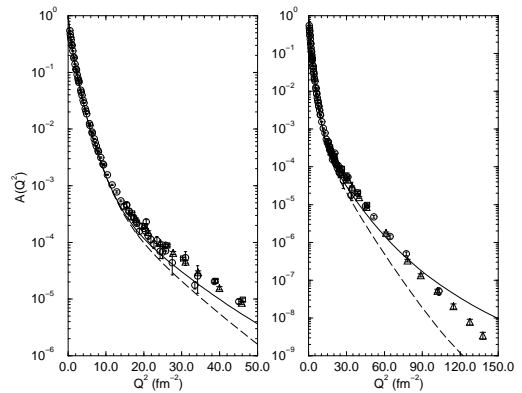


FIG. 3. The deuteron structure function A . The left panel is an enlarged version of the right one. In both the dashed line is the impulse approximation result, and the solid line is the result with the $\rho\pi\gamma$ MEC included. The experimental data of Refs. [28,29] are denoted by the open circles, while that of Refs. [26,27] are represented by triangles and squares.

We see clearly in the left panel of Fig. 3 that the impulse approximation underpredicts the A data for $Q^2 = 1 - 2 \text{ GeV}^2$. Much of this lack of strength is made up for by the $\rho\pi\gamma$ MEC, which gives a curve that reproduces the data in the region $Q^2 = 2 - 4 \text{ GeV}^2$. However, this MEC calculation then *overpredicts* the JLab data at large Q^2 . Our $\rho\pi\gamma$ MEC contribution to A scales as Q^{-20} when Q is large, which is consistent with perturbative QCD. The failure of our calculation to describe the data for $Q^2 > 4 \text{ GeV}^2$ implies that the $\rho\pi\gamma$ mechanism is too strong at large Q in the present model.

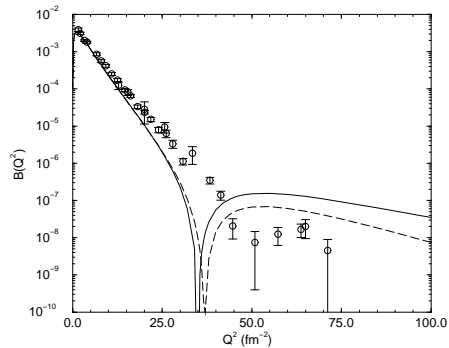


FIG. 4. The deuteron structure function B . The experimental data are given by the open circles. The dashed and solid lines represent impulse approximation and $\rho\pi\gamma$ MEC calculations.

As seen in Fig. 4 the extant experimental data for B (which, as yet, includes no JLab data) [29,30] are even less well-described. Already at $Q^2 < 1 \text{ GeV}^2$ there is significant disagreement between our calculation and the data. This disagreement is worsened by the inclusion of the relativistic version of the $\rho\pi\gamma$ MEC: an effect also seen in the calculations of Ref. [7]. There is a significant variation in results for this observable at $Q^2 = 1 - 2 \text{ GeV}^2$

in non-relativistic formulations of this problem, partly because in this regime B is sensitive to currents associated with the short-range piece of the NN interaction. These currents, as well as other mechanisms not in our model, could play a key role in reproducing the B data.

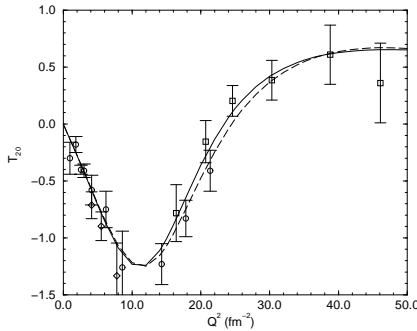


FIG. 5. The tensor-polarization observable T_{20} . The older experimental data are denoted by the open circles, the recent NIKHEF data of Bouwhuis *et al.* by diamonds, and the JLab data of Beise *et al.* by squares. The dashed and solid line represent impulse approximation and $\rho\pi\gamma$ MEC calculations.

On the other hand, Fig. 5 shows that the T_{20} data of Refs. [31,32] is well-described by our approach out to $Q^2 \approx 2 \text{ GeV}^2$. This observable is fairly insensitive to some of the dynamics which plays a role in A and B (e.g. the single-nucleon form factors). However, it is quite sensitive to relativistic effects (see, for instance [2,10]), so it is gratifying that our approach reproduces the data, especially that of Ref. [32] at large Q^2 , so well.

ACKNOWLEDGMENTS

We thank E. J. Beise and M. Petratos for useful conversations. We are also grateful to the U. S. Department of Energy, Nuclear Physics Division, for its support under grants DE-FG02-93ER-40762 and DE-FG03-97ER41014.

[1] R. Schiavilla and D. O. Riska, Phys. Rev. C **43**, 437 (1991).
[2] R. B. Wiringa, V. G. J. Stoks, and R. Schiavilla, Phys. Rev. C **51**, 38 (1995).
[3] D. R. Phillips and S. J. Wallace, Phys. Rev. C **54**, 507 (1996).
[4] D. R. Phillips and S. J. Wallace, Few-body Syst. **24**, 175 (1997).
[5] D. R. Phillips, S. J. Wallace, and N. K. Devine, Phys. Rev. C **58**, 2261 (1998).
[6] R. G. Arnold, C. E. Carlson, and F. Gross, Phys. Rev. C **21**, 1426 (1980).
[7] E. Hummel and J. A. Tjon, Phys. Rev. Lett. **63**, 1788 (1989); Phys. Rev. C **42**, 423 (1990); *ibid.* **49**, 21 (1994).

[8] J. W. van Orden, N. K. Devine, and F. Gross, Phys. Rev. Lett. **75**, 4369 (1995).
[9] P. L. Chung, W. N. Polyzou, F. Coester, and B. D. Keister, Phys. Rev. C **37**, 2000 (1988).
[10] J. Carbonell and V. A. Karmanov, nucl-th/9902053.
[11] J. Fleischer and J. A. Tjon, Nucl. Phys. **B84**, 375 (1975); Phys. Rev. D **15**, 2537 (1977); *ibid.* **21**, 87 (1980).
[12] F. Gross, Phys. Rev. C **26**, 2203 (1982).
[13] E. E. Salpeter, Phys. Rev. **87**, 328 (1952).
[14] A. A. Logunov and A. N. Tavkhelidze, Nuovo Cim. **29**, 380 (1963).
[15] A. N. Kvinikhidze and B. Blankleider, Few-Body Syst. Suppl. **7**, 294 (1994).
[16] A. Klein, Phys. Rev. **90**, 1101 (1953); *ibid.* **94**, 1052 (1954).
[17] V. B. Mandelzweig and S. J. Wallace, Phys. Lett. B. **197**, 469 (1987); S. J. Wallace and V. B. Mandelzweig, Nucl. Phys. **A503**, 673 (1989).
[18] D. R. Phillips, M. C. Birse, and S. J. Wallace, Phys. Rev. C **55**, 1937 (1997).
[19] F. Gross and D. O. Riska, Phys. Rev. C **36**, 1928 (1987).
[20] D. O. Riska, Prog. Part. Nucl. Phys. **11**, 199 (1984).
[21] J. Carlson and R. Schiavilla, Rev. Mod. Phys. **70**, 743 (1998).
[22] R. Machleidt, Adv. Nucl. Phys. **19**, 189 (1989).
[23] V. G. J. Stoks, R. A. M. Klomp, C. P. F. Terheggen, and J. J. de Swart, Phys. Rev. C **49**, 2950 (1994).
[24] R. Machleidt, F. Sammarruca, and Y. Song, Phys. Rev. C **53**, 1483 (1996).
[25] P. Mergell, U.-G. Meissner, and D. Drechsel, Nucl. Phys. **A596**, 367 (1996).
[26] L. C. Alexa *et al.*, Phys. Rev. Lett. **82**, 1374 (1999).
[27] D. Abbott *et al.*, Phys. Rev. Lett. **82**, 1379 (1999).
[28] J. E. Elias *et al.*, Phys. Rev. **177**, 2075 (1969); R. G. Arnold *et al.*, Phys. Rev. Lett. **35**, 776 (1975); S. Platchkov *et al.*, Nucl. Phys. **A510**, 740 (1990).
[29] G. G. Simon, C. Schmitt, and V. H. Walther, Nucl. Phys. **A364**, 285 (1981); R. Cramer *et al.*, Z. Phys. C **29**, 513 (1985).
[30] S. Auffret *et al.*, Phys. Rev. Lett. **54**, 649 (1985); P. Bosted *et al.*, Phys. Rev. C **42**, 38 (1990).
[31] M. E. Schulze *et al.*, Phys. Rev. Lett. **52**, 597 (1984); V. F. Dmitriev *et al.*, Phys. Lett. B. **157**, 143 (1985); B. B. Voitsekhovskii *et al.*, JETP Lett. **43**, 733 (1986); R. Gilman *et al.*, Phys. Rev. Lett. **65**, 1733 (1990); M. Ferro-Luzzi *et al.*, Phys. Rev. Lett. **77**, 2630 (1996); M. Bouwhuis *et al.* Phys. Rev. Lett. **82**, 3755 (1999).
[32] I. The *et al.*, Phys. Rev. Lett. **67**, 173 (1991); E. J. Beise *et al.* Few-Body Syst. Suppl. **10**, 315 (1999).